View metadata, citation and similar papers at core.ac.uk

brought to you by CORE

provided by Elsevier - Publisher Connector

© 2009 BY THE AMERICAN COLLEGE OF CARDIOLOGY FOUNDATION
ISSN 1936-878X/09/$36.00
PUBLISHED BY ELSEVIER INC.
DOI:10.1016/j.jcmg.2008.12.019

Prospective Electrocardiogram-Gated Delayed Enhanced Multidetector Computed Tomography Accurately Quantifies Infarct Size and Reduces Radiation Exposure

Hyuk-Jae Chang, MD, PhD, Richard T. George, MD, Karl H. Schuleri, MD, Kristine Evers, Kakuya Kitagawa, MD, PhD, João A. C. Lima, MD, Albert C. Lardo, PhD

Baltimore, Maryland

OBJECTIVES This study sought to determine whether low-dose, prospective electrocardiogram (ECG)-gated delayed contrast-enhanced multidetector computed tomography (DCE-MDCT) can accurately delineate the extent of myocardial infarction (MI) compared with retrospective ECG-gated DCE-MDCT.

BACKGROUND For defining the location and extent of MI, DCE-MDCT compares well with delayed enhanced cardiac magnetic resonance. However, the addition of a delayed scan requires additional radiation exposure to patients. The MDCT protocols using prospective ECG gating can substantially reduce effective radiation dose exposure, but these protocols have not yet been applied to infarct imaging.

METHODS Ten porcine models of acute MI were imaged 10 days after MI using prospective and retrospective ECG-gated DCE-MDCT (64-slice) 10 min after a 90-ml contrast bolus. The MDCT images were analyzed using a semiautomated signal intensity threshold technique. Infarct size, signal-to-noise (SNR) ratios, contrast-to-noise (CNR) ratios, and image quality metrics were compared using the 2 ECG-gating techniques.

RESULTS Infarct volume measurements obtained by both methods were strongly correlated ($R = 0.93$, $p < 0.001$) and in good agreement (mean difference: -0.46 ml $\pm$ 4.00%). Compared with retrospective ECG gating, estimated radiation dosages were markedly reduced with prospective ECG gating (930.1 $\pm$ 62.2 mGy$\times$cm vs. 42.4 $\pm$ 2.3 mGy$\times$cm, $p < 0.001$). The SNR and CNR of infarcted myocardium were somewhat lower for prospective gated images (22.0 $\pm$ 11.0 vs. 16.3 $\pm$ 7.8 and 8.8 $\pm$ 5.3 vs. 7.0 $\pm$ 3.9, respectively; $p < 0.001$). However, all of the examinations using prospective gating protocol achieved sufficient diagnostic image quality for the assessment of MI.

CONCLUSIONS Prospective ECG-gated DCE-MDCT accurately assesses infarct size compared with retrospective ECG-gated DCE-MDCT imaging. Although SNR and CNR of infarct were significantly higher for the retrospective gated protocol, prospective ECG-gated DCE-MDCT can provide high-resolution imaging of MI, while substantially lowering the radiation dose. (J Am Coll Cardiol Img 2009;2:412–20)
© 2009 by the American College of Cardiology Foundation

From the Department of Medicine, Division of Cardiology, Johns Hopkins University School of Medicine, Baltimore, Maryland. This study was supported, in part, by research grants from Toshiba Medical Systems Co., Ltd., Tokyo, Japan. Dr. George was supported by the Donald W. Reynolds Cardiovascular Research Center at Johns Hopkins University. The terms of this arrangement are managed by Johns Hopkins University in accordance with its conflict of interest policies. Drs. Chang and George contributed equally to this paper.

Manuscript received July 23, 2008; revised manuscript received December 11, 2008, accepted December 24, 2008.

The ability to distinguish dysfunctional but viable myocardium from nonviable tissue after myocardial ischemia has important implications for the therapeutic management of patients with coronary artery disease (CAD) (1,2). The assessment of both myocardial viability and infarct morphology using delayed contrast-enhancement (DCE)-cardiac magnetic resonance

See page 421

(CMR) has been well validated over the past several years (3,4); however, the limited spatial resolution of CMR has the potential to overestimate infarct size because of partial volume effects (5), and technique is still time-consuming to exclude its application in the setting of acute chest pain. Furthermore, with the proliferation of intracardiac devices (i.e., implantable cardioverter-defibrillators and biventricular pacers), alternatives to DCE-CMR are required in this population of patients, who are potential candidates for viability imaging.

The potential to visualize nonviable myocardium using computed tomography (CT) was first reported in late 1970s (6,7). Because iodinated contrast agents for CT show similar delayed contrast kinetics as gadolinium-based CMR contrast agents (8) and new-generation detectors are providing images with unsurpassed spatial resolution, the direct assessment of myocardial viability by means of DCE multidetector computed tomography (MDCT) has evoked increasing interest and initial results are promising. Recently, we showed that the spatial extent of acute and healed myocardial infarction (MI) can be determined and quantified accurately with DCE-MDCT (9). However, increasing the X-ray exposure with additional late scans is a major obstacle to the widespread use of MDCT for this application.

So far, infarct detection by MDCT has most often been based on the description of perfusion deficits during the first pass of contrast. The MDCT first-pass imaging correlates well with infarct size in non-reperfused MI (10,11); however, in the setting of reperfusion, it shows insufficient accuracy and significant underestimation of infarct size (12,13).

Several studies reported various low-dose DCE-MDCT protocols based on modulation of tube current and/or reductions in tube voltage (14–16). However, these methods come at the cost of greater image noise, and dose reductions were not enough to apply DCE-MDCT into routine clinical practice, when combined with coronary computed tomography angiography (CCTA).

More recently, new CCTA acquisition protocols have been proposed with prospective electrocardiogram (ECG) gating (17). With this technique, radiation is only administered at predefined time points of the cardiac cycle, rather than the entire cardiac cycle as in the case of retrospective ECG-gated helical MDCT acquisition. The former is associated with a substantial reduction of radiation dose without compromise of diagnostic image quality.

Accordingly, the purpose of the present study was to explore the hypothesis that low-radiation DCE-MDCT viability imaging with prospective ECG gating is accurate for the measurement of infarct size and microvascular obstruction (MVO) compared with high-dose retrospective ECG-gated DCE-MDCT imaging.

ABBREVIATIONS AND ACRONYMS

CAD = coronary artery disease
CCTA = coronary computed tomographic angiography
CI = confidence interval
CNR = contrast-to-noise ratio
CMR = cardiac magnetic resonance
CT = computed tomography
DCE = delayed contrast-enhancement
ECG = electrocardiogram
LAD = left anterior descending
LV = left ventricle/ventricular
MDCT = multidetector computed tomography
MI = myocardial infarction
MVO = microvascular obstruction
ROI = region of interest
SI = signal intensity
SNR = signal-to-noise ratio

METHODS

Animal preparation. All animal studies were approved by the Johns Hopkins University Institutional Animal Care and Use Committee and comply with the Guide for the Care and Use of Laboratory Animals (National Institutes of Health publication no. 80-23, revised 1985).

Myocardial infarction was created by temporary balloon occlusion of the left anterior descending (LAD) coronary artery for 120 min, followed by reperfusion. Ten Göttingen minipigs (Marshall BioResources, North Rose, New York) (mean weight 28 ± 3 kg) were subjected to induction of anesthesia with ketamine (35 mg/kg intramuscularly), and initially anesthesia was achieved with pentobarbital (20 to 60 mg/kg intravenously). Minipigs were intubated and mechanically ventilated with inhaled isoflurane during catheterization and MDCT scanning. A midline neck incision was made, and the right carotid artery was cannulated with an 8-F sheath. Heparin 5,000 U was administered intravenously. Left ventriculogram was performed with either a 7-F pigtail catheter with side holes or a Judkins right 4 guide catheter in both the left anterior oblique views. The left coronary artery was cannulated with a Judkins right 4 or hockey stick guiding catheter, and a baseline coronary angiogram was obtained to show the patency of artery. Then, a 0.014-inch angioplasty guidewire was inserted into the LAD under fluoroscopic guidance and 2.5 × 12-mm Maverick balloon (Boston Scientific, Natick, Massachusetts)

Table 1. Comparison of Parameters According to Scan Protocols

	Prospectively Gated	Retrospectively Gated
Scanning		
Detector collimation, mm	4 × 3	64 × 0.5
Tube voltage, kV	120	120
Tube current, mA	150	400
Gantry rotation, s	0.4	Variable
Helical pitch	—	Variable
ECG triggering, percent of R-R interval	50	—
Field of view, mm	120	120
Reconstruction	Half	Segmental
Convulation kernel	FC 43	FC 43
Percent of R-R interval	50	50
Slice thickness, mm	3	3

ECG = electrocardiographic.

was inflated to 4 atm just distal to the second diagonal branch of the LAD. Complete cessation of flow in the LAD was confirmed by angiography. The balloon was left inflated for 120 min with an intravenous lidocaine infusion throughout this time. After balloon deflation, restoration of flow in the LAD was confirmed by angiography and any spasm of the coronary artery was treated with intracoronary nitroglycerin 100 μg. Repeat left ventriculogram confirmed the presence of an anterior wall myocardial infarction. The catheters and sheath were removed, and the carotid artery ligated.

MDCT imaging and reconstruction. The MDCT imaging was performed with a 0.5 mm × 64-detector scanner (Aquilion 64, Toshiba Medical Systems Corporation, Otawara, Japan). Animals received intravenous metoprolol (2 to 5 mg) and amiodarone (50 to 150 mg) to achieve a heart rate <100 beats/min for delayed-enhancement studies. Mean heart rate during the MDCT examination was 96 ± 8 beats/min. After scout acquisition and slice prescription, a 90-ml bolus of iodixanol (Visipaque 320, Amersham Health, Amersham, United Kingdom) was injected intravenously at a rate of 5 ml/s, followed by a 30-ml saline chaser. During image acquisition, mechanical ventilation was suspended and delayed enhanced images were acquired 10 min after contrast delivery. Immediately after scanning with a prospective ECG-gated MDCT protocol, which was developed for calcium score scan, a retrospectively gated scan was performed with preset parameters as in Table 1. The mean time interval between both scans was 45 ± 15 s (Fig. 1).

After acquisition of the dataset, prospectively and retrospectively gated scan images were reconstructed at a 3-mm slice thickness using identical

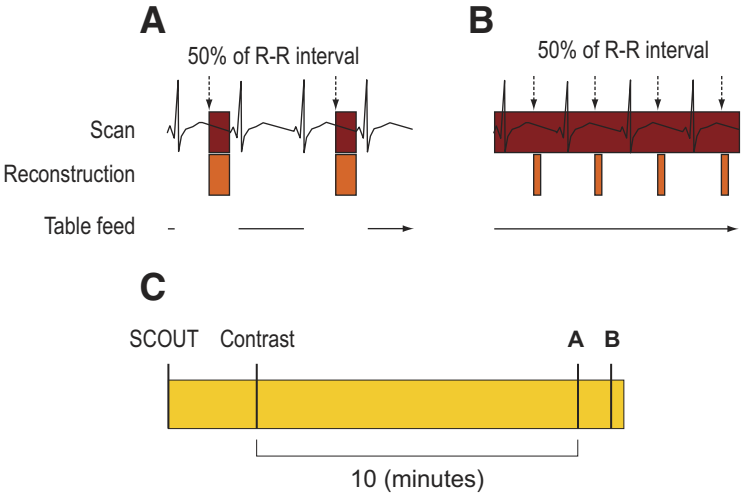

Figure 1. Experimental Prospective and Retrospective ECG-Gated MDCT Protocol

(A) Prospective electrocardiogram (ECG)-gated protocols prospectively trigger the start of axial scanning at predefined phase of the R-R interval, in this case 50%. Imaging occurs every other heartbeat with table movement occurring during the heartbeat between 2 scans. Half scan techniques gave an exposure time of approximately 0.3 s for a scanner with a 0.5-s gantry rotation time. All of the dataset acquired during scan was used to image reconstruction. **(B)** Retrospective ECG-gated protocol using continuous table feeding and scanning. Using this method, image data throughout the R-R interval is acquired over several heartbeats. Using retrospective ECG reconstruction methods, images can be reconstructed at any specific phase of the R-R interval, in this case 50%. **(C)** Experimental multidetector computed tomography (MDCT) protocol timeline. After scout imaging, iodinated contrast was infused; followed 10 min later by delayed MDCT imaging sequentially with prospective and retrospective ECG-gated protocols.

convolution kernel (FC 43) by half-segment and multisegment reconstruction algorithms, respectively. The source images on the same phase of the cardiac cycle with prospectively gated scan were selected for reconstruction from retrospectively gated scan (Table 1). For exposure dose calculation, an acrylic phantom with a diameter of 32 cm was scanned with a 32-cm field of view to measure weighted computed tomography dose index (CTDIw). A calibrated ion chamber dosimeter was used for measurement. The result showed that the normalized CTDIw (nCTDIw) per 100 mAs at 120 kV was 9.4 mGy/100 mAs. Based on this result, the exposure dose for the following scan conditions is calculated based on the scan conditions shown in Table 1 (18).

Image analysis. The reconstructed data set was then transferred to a custom cardiac software package (Cine Display Application, GE Medical Systems, Milwaukee, Wisconsin) for image analysis.

Using hand planimetry, after definition of endocardial and epicardial contours of left ventricle (LV), normal myocardial signal intensity (SI) was determined by drawing a region of interest (ROI) in the myocardium remote from the infarct in each slice. These results were used to define a hyperenhancement SI threshold as myocardium having an SI 1 SD above the mean SI of the remote region. Infarct area was then calculated using a step-based algorithm to: 1) detect voxels within the defined SI range; 2) check for voxel continuity in the X, Y, and Z directions; 3) generate clusters of voxels that meet the hyperenhancement definition; and 4) define the hyperenhancement as the largest cluster detected. Using this method, the software determined the mean SI of the hyperenhancement in Hounsfield units and calculated total infarct volume and total percent volume. MVO was defined as the hypoenhanced regions within the hyperenhanced area (Fig. 2). The MDCT images were also analyzed by 2 independent experienced operators to calculate interobserver and intraobserver agreements in a random subset of 5 animals.

In each animal, visually matching corresponding subsets of 5 image slices were chosen for comparison of quantitative and qualitative assessments of

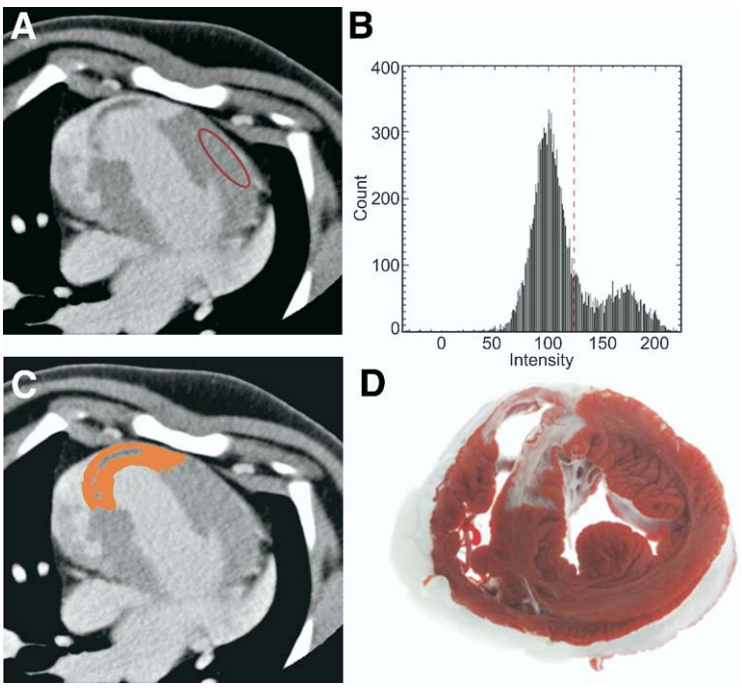

Figure 2. Method of Image Analysis

(A) Infarction area was defined as those with a signal intensity (SI) higher than 1 SD above the mean SI of remote normal myocardium **(red)**. **(B)** Based on graphics displayed by SI histogram thresholding, infarct was calculated using a step-based algorithm to detect voxels within the defined SI range in the 3 dimensions and **(C)** to define clusters of voxels that meet the hyperenhancement definition **(orange)**. Using this method, the software determined the mean SI of the hyperenhancement in Hounsfield units and calculated total infarct volume and total percent volume. Microvascular obstruction was defined as the hypoenhanced regions within the hyperenhanced area. **(D)** Histopathologic staining of infarct morphology with a triphenyl tetrazolium-stained slice showing a anteroseptal infarct.

image quality according to scan protocols. The SIs were measured on the raw-data images by drawing 10-mm^2 ROI in LV blood pool (SI_{blood}), infarct (SI_{inf}), and normal myocardium (SI_{myo}). The signal-to-noise ratio (SNR) was defined as the ratio of mean SI in the ROIs to the SD of the SI in the air (i.e., noise) (SD_{noise}) lateral to the thorax. The contrast-to-noise ratio (CNR) was calculated according to the following formula (18): $CNR = (SI_{inf} - SI_{myo}) / SD_{noise}$. The quality of image was assessed on a 4-point scale: 1) indicated very unsatisfactory and not useful for diagnostic purposes; 2) unsatisfactory, with serious compromise of diagnostic image quality; 3) satisfactory, with good diagnostic image quality; and 4) very satisfactory, with very good diagnostic image quality (18).

Statistical analysis. Agreement of the results was determined by the Pearson correlation coefficient (19) and Bland-Altman method calculated as mean ± SD difference between the 2 methods at 95% confidence interval (CI) (20). According to the normality of distribution, paired *t* test (21) or Wilcoxon signed rank test (22) was performed to determine whether there were significant differences in parameters between scan protocols. Intraobserver and interobserver variance was calculated as mean difference ± SD. Statistical significance was defined as a 2-sided probability value <0.05, and all analyses were performed using MedCalc for Windows, version 8.1.1.0 (MedCalc Software, Mariakerke, Belgium).

RESULTS

The MDCT scan images were successfully obtained in all animals from both protocols. The DCE in the infarct territory was confirmed in all animals (Fig. 3). Total LV myocardial volumes as measured by prospective scan did not differ (mean absolute difference: 0.54 ± 5.81%) and linearly correlated with ones of retrospective scan (R = 0.69, 95% CI: −0.10 to 0.92, p = 0.03).

Infarct and MVO volumes and their percent volume ratios of total LV myocardium as measured in each protocol also did not differ, and prospective scan showed only tendency to overestimation of MVO area when compared with retrospective scan (Table 2).

Comparison of infarct and MVO percent volumes between both protocols showed good correlations and only small mean differences (−0.46 ± 4.00% and −0.99 ± 1.45%, respectively) (Fig. 4).

For retrospectively gated data sets, interobserver and intraobserver measurements of infarct percent volumes were closely correlated (R = 0.97, 95% CI: 0.59 to 1.00, p = 0.01, and R = 0.98, 95% CI: 0.67 to 1.00, p = 0.01, respectively) and mean differences in infarct volumes were small (1.98 ± 3.10%

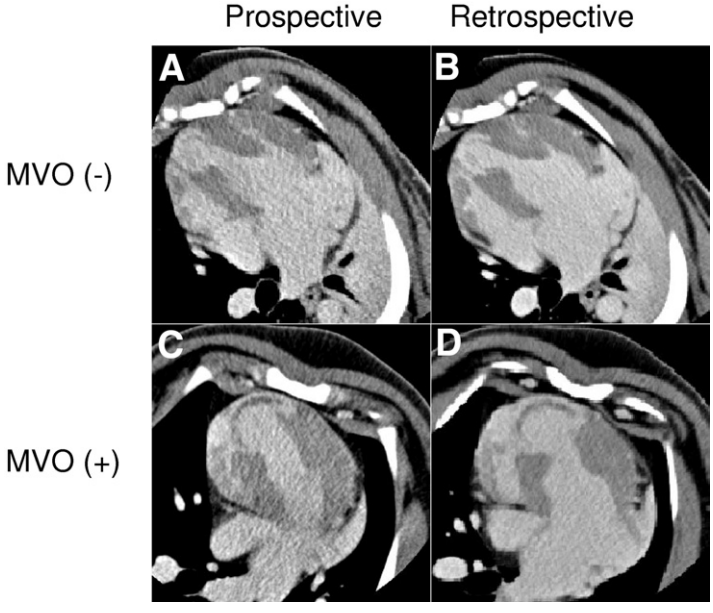

Figure 3. Comparison of Prospective and Retrospective ECG-Gated MDCT Images 10 Min After Contrast Injection

Visualization of myocardial infarction 10 days after balloon occlusion-reperfusion injury in retrospective and prospective scans, with or without microvascular obstruction (MVO). Abbreviations as in Figure 1.

Table 2. Comparison of Volume of Interests According to Scan Protocols (n = 10)

	Retrospective Scan	Prospective Scan	p Value
LV myocardium, total, ml	54.99 ± 6.89	56.02 ± 7.80	0.65
Infarct, ml	13.11 ± 3.90	13.67 ± 4.65	0.22
Percent infarct	24.2 ± 8.4	24.7 ± 8.9	0.68
MVO, ml	0.97 ± 0.70	1.51 ± 1.07	0.05
Percent MVO	1.8 ± 1.3	2.7 ± 2.1	0.06

Values are expressed as mean ± SD.
LV = left ventricle; MVO = microvascular obstruction.

and 0.45 ± 2.44%, respectively). Similar results were obtained for prospectively gated acquisitions (R = 0.96, 95% CI: 0.55 to 1.00, p = 0.01, and R = 0.98, 95% CI: 0.62 to 1.00, p = 0.005; mean differences, 2.40 ± 3.30% and 0.31 ± 3.58%, respectively).

Although the SNR and CNR of infarct were somewhat higher for the retrospective technique, prospective ECG-gated DCE-MDCT provided high-resolution imaging of MI with lowering the radiation dose (930.1 ± 62.2 mGy×cm vs. 42.4 ± 2.3 mGy×cm, p < 0.001). On a slice by-slice analysis, the SIs of LV blood pool, normal myocardium, and infarcted myocardium were not different between both methods (Table 3).

The SNRs of infarct and normal myocardium were lower in scan images using the prospective gating protocol, and contrast-to-noise ratio between infarct and normal myocardium was also reduced by the prospective gating protocol. However, in qualitative analysis, all the examinations using retrospective ECG gating protocol have diagnostic image quality for the assessment of myocardial contrast change (52%: good, 48%: excellent on a per-slice analysis; 50%: good, 50%: excellent on a per-subject analysis) and all the examinations using prospective gating protocol were comparatively lower but also achieved sufficient diagnostic image quality (62%: good, 38%: excellent on a per-slice analysis, p < 0.001; 70%: good, 30%: excellent on a per-subject analysis, p = 0.04).

DISCUSSION

The major finding of the present study is that prospective ECG-gated DCE-MDCT myocardial imaging can accurately quantify nonviable and viable myocardium after myocardial infarction as current retrospective ECG-gated DCE-MDCT im-

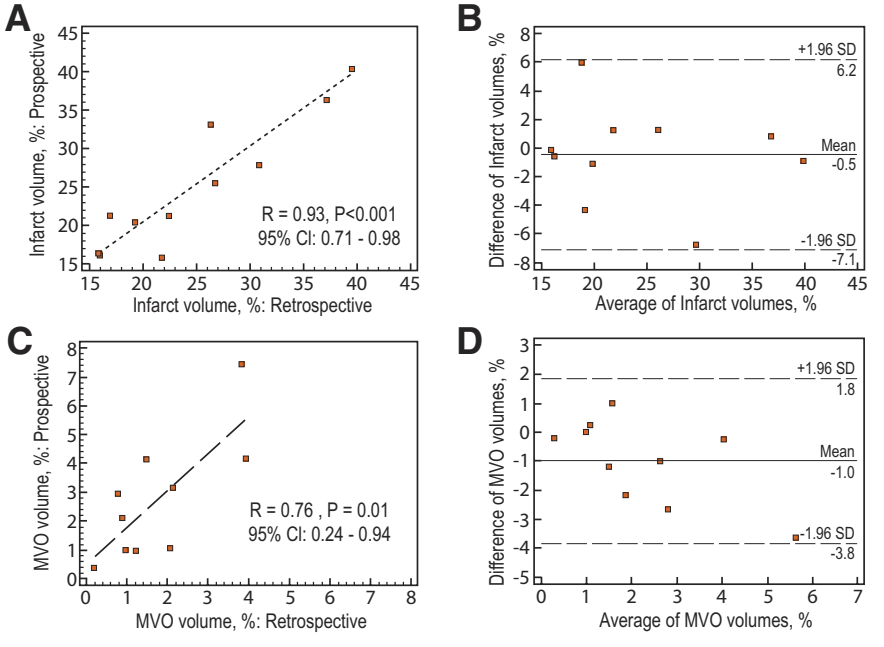

Figure 4. Correlations and Quality Control Plots for Infarct and MVO Percent Volume Between Prospective and Retrospective ECG-Gated MDCT Protocols

Correlation analysis using scatter diagram and regression line of infarct percent volume **(A)** and MVO percent volume **(B)** between the 2 protocols. Quality control plots using Bland-Altman analysis of the agreement of infarct percent volume **(C)** and MVO percent volume **(D)** between the 2 protocols. Abbreviations as in Figures 1 and 3.

Table 3. Differences in Parameters of Quantitative Image Analysis According to Scan Protocols (n = 50, 5 Slices per Animal)

	Prospective Scan	Retrospective Scan	p Value
Signal intensity, HU			
LV blood pool	190.4 ± 26.0	186.2 ± 31.4	0.13
Infarct	184.2 ± 24.3	179.6 ± 31.1	0.34
Normal myocardium	105.6 ± 20.1	108.0 ± 18.6	0.48
SD_{noise}, HU	12.7 ± 3.9	9.4 ± 3.1	<0.001
SNR_{myo}	9.3 ± 4.5	13.2 ± 6.4	<0.001
SNR_{inf}	16.3 ± 7.8	22.0 ± 11.0	<0.001
CNR	7.0 ± 3.9	8.8 ± 5.3	0.01

Values are expressed as mean ± SD Wilcoxon signed rank test.
CNR = contrast-to-noise ratio; LV = left ventricle; SNR_{inf} = signal-to-noise ratio of infarct; SD_{noise} = standard deviation of the signal intensity in the air; SNR_{myo} = signal-to-noise ratio of normal myocardium.

aging and also significantly reduces the amount of radiation exposure.

Almost 30 years ago, the potentials of computed tomography for the detection of MI were reported (6–8), and since then, improvement of MDCT technology permits sufficient spatial and temporal resolution to define myocardial viability. Due to concerns about increasing X-ray exposure with additional late scans; however, infarct detection by MDCT has been based on the appearance of perfusion deficits during the first pass of contrast. Hoffmann et al. (10) performed 4-slice MDCT in a pig model of nonreperfused MI and showed a good correlation between histomorphometric infarct and MDCT regions of hypoenhancement. In the setting of reperfusion (12,13), however, MDCT first-pass imaging shows insufficient accuracy and significant underestimation of infarct size, which have become much more common after the introduction of reperfusion therapy.

The DCE-MDCT can determine and accurately quantify MI by well-delineated hyperenhanced regions within certain time intervals after contrast injection, whereas regions of MVO are characterized by hypoenhancement on early imaging in a time-dependent manner (9,23). Furthermore, iodine concentration on the infarct region reaches a maximum very quickly (5 to 10 min) after contrast injection; therefore, the single contrast bolus can be used to acquire both CCTA and DCE-MDCT to enhance nonviable myocardium. The assessment of both myocardial viability and infarct morphology, in conjunction with current high-resolution coronary artery imaging, represents an undisputed advantage of MDCT over other competing imaging technologies and has important implications for comprehensive assessment of the patients with CAD and MI. Hence, establishment of MDCT protocols with a lower radiation dose while maintaining suitable image quality is an essential prerequisite to assess myocardial viability as a part of a comprehensive study.

Initial studies for the practicability of MDCT viability imaging have been performed with standard 120 kV and 400 to 800 mAs full-dose protocols (15), but there are also promising results with lower-dose late-phase CT scans. Brodoefel et al. (14) reported that myocardial viability can accurately be assessed by MDCT at 80 kV. Closer to the K-edge of iodine, a tube voltage of 80 kV achieves a more optimal absorption of radiation and hence has the potential to allow better contrast enhancement. However, this comes at the cost of greater image noise. Therefore, prior studies have used high tube current (800 mAs), which lowers the radiation dose by only 65% when compared with standard acquisition parameters. In practice, using 80 kV, the image noise was shown to exponentially increase in thoracic imaging of patients weighing more than 75 kg. Therefore, weight issues also remain a considerable limitation to the exclusive use of low kilovoltage protocols in clinical routine practice (24).

More recently, a new CCTA acquisition protocol has been introduced that utilizes prospective ECG gating (17). Prospective ECG-gated protocols limit radiation dose exposure to only a small portion of the R-R interval, thus significantly reducing X-ray exposure time to patients. This is in contrast to retrospective ECG-gated protocols during helical MDCT imaging that continuously expose patients to radiation throughout the R-R interval over 5 to 10 heartbeats. The former is likely to be associated with a substantial (90%) reduction of radiation dose. In the present study, we used the prospective ECG-gated protocol that we currently use to perform calcium scoring (120 kV/150 mA) and compared with our commonly used 64-slice CCTA protocol (120 kV/400 mA). Although the signal intensity of infarct and normal myocardium were not different between protocols, there was a decrease in the SNRs of infarct and normal myocardium using the prospective ECG-gated protocol, primarily attributed to its lower tube current and longer data windows used for image reconstruction (half vs. segmental scan reconstruction). However, in the qualitative analysis, all the examinations using the prospective ECG-gated protocol achieved sufficient diagnostic image quality for the assessment of myocardial contrast change. In addition to a decrease in dose caused by the prospective nature

of the acquisition, there is a further decrease attributable to the use of a wider collimation. Nieman et al. (25) showed a decrease in radiation exposure with a wider detector collimation (24 × 1.2 mm) and lower tube output (100 kV, 800 mAs). However, the calculated radiation dose was 4.5 ± 2.4 mSv, which was still 62% of their standard acquisition protocol. In our study, we showed that prospective ECG-gated DCE-MDCT can provide a substantial radiation dose reduction and seems to be feasible without sacrificing diagnostic accuracy.

Study limitations. In the present study, we did not provide CMR or histopathological correlation with infarcted tissue as defined by DCE-MDCT. However, our previous experimental work (9) did show that the spatial extent of MI can be quantified accurately with retrospective ECG-gated DCE-MDCT imaging. The contrast injection used in the study for 30-kg pigs in average is approximately equivalent to a double contrast dose for an average-sized patient. Such a dose (90 ml) was selected to ensure that the contrast material was not a limiting factor and tissue uptake was maximized to define the ROI accurately.

CONCLUSIONS

Prospective ECG-gated MDCT imaging can accurately assess infarct and MVO size when compared with retrospective ECG-gated MDCT imaging. Although SNR and CNR of infarct were significantly higher in retrospective ECG-gated protocol, prospective ECG-gated DCE-MDCT can provide high-resolution imaging of MI while lowering the radiation dose from 930.1 to 42.4 mGy×cm.

Reprint requests and correspondence: Dr. Albert C. Lardo, Johns Hopkins University School of Medicine/Division of Cardiology, 1042 Ross Building, 720 Rutland Avenue, Baltimore, Maryland 21205. *E-mail: al@jhmi.edu.*

REFERENCES

1. Pagley PR, Beller GA, Watson DD, Gimple LW, Ragosta M. Improved outcome after coronary bypass surgery in patients with ischemic cardiomyopathy and residual myocardial viability. Circulation 1997;96:793–800.
2. Bax JJ, Schinkel AF, Boersma E, et al. Early versus delayed revascularization in patients with ischemic cardiomyopathy and substantial viability: impact on outcome. Circulation 2003;108 Suppl 1:II39–42.
3. Gerber BL, Rochitte CE, Melin JA, et al. Microvascular obstruction and left ventricular remodeling early after acute myocardial infarction. Circulation 2000;101:2734–41.
4. Wu KC, Lima JA. Noninvasive imaging of myocardial viability: current techniques and future developments. Circ Res 2003;93:1146–58.
5. Fieno DS, Kim RJ, Chen EL, Lomasney JW, Klocke FJ, Judd RM. Contrast-enhanced magnetic resonance imaging of myocardium at risk: distinction between reversible and irreversible injury throughout infarct healing. J Am Coll Cardiol 2000;36:1985–91.
6. Gray WR, Buja LM, Hagler HK, Parkey RW, Willerson JT. Computed tomography for localization and sizing of experimental acute myocardial infarcts. Circulation 1978;58:497–504.
7. Higgins CB, Siemers PT, Schmidt W, Newell JD. Evaluation of myocardial ischemic damage of various ages by computerized transmission tomography. Time-dependent effects of contrast material. Circulation 1979;60:284–91.
8. Higgins CB, Siemers PT, Newell JD, Schmidt W. Role of iodinated contrast material in the evaluation of myocardial infarction by computerized transmission tomography. Invest Radiol 1980;15:S176–82.
9. Lardo AC, Cordeiro MA, Silva C, et al. Contrast-enhanced multidetector computed tomography viability imaging after myocardial infarction: characterization of myocyte death, microvascular obstruction, and chronic scar. Circulation 2006;113:394–404.
10. Hoffmann U, Millea R, Enzweiler C, et al. Acute myocardial infarction: contrast-enhanced multi-detector row CT in a porcine model. Radiology 2004;231:697–701.
11. Mahnken AH, Bruners P, Katoh M, Wildberger JE, Gunther RW, Buecker A. Dynamic multi-section CT imaging in acute myocardial infarction: preliminary animal experience. Eur Radiol 2006;16:746–52.
12. Mahnken AH, Koos R, Katoh M, et al. Assessment of myocardial viability in reperfused acute myocardial infarction using 16-slice computed tomography in comparison to magnetic resonance imaging. J Am Coll Cardiol 2005;45:2042–7.
13. Nikolaou K, Knez A, Sagmeister S, et al. Assessment of myocardial infarctions using multidetector-row computed tomography. J Comput Assist Tomogr 2004;28:286–92.
14. Brodoefel H, Klumpp B, Reimann A, et al. Late myocardial enhancement assessed by 64-MSCT in reperfused porcine myocardial infarction: diagnostic accuracy of low-dose CT protocols in comparison with magnetic resonance imaging. Eur Radiol 2007;17:475–83.
15. Sigal-Cinqualbre AB, Hennequin R, Abada HT, Chen X, Paul JF. Low-kilovoltage multi-detector row chest CT in adults: feasibility and effect on image quality and iodine dose. Radiology 2004;231:169–74.
16. Mahnken AH, Bruners P, Muhlenbruch G, et al. Low tube voltage improves computed tomography imaging of delayed myocardial contrast enhancement in an experimental acute myocardial infarction model. Invest Radiol 2007;42:123–9.
17. Husmann L, Valenta I, Gaemperli O, et al. Feasibility of low-dose coronary CT angiography: first experience with prospective ECG-gating. Eur Heart J 2008;29:191–7.
18. Morin RL, Gerber TC, McCollough CH. Radiation dose in computed tomography of the heart. Circulation 2003;107:917–22.
19. Thurnher SA, Capelastegui A, Del Olmo FH, et al. Safety and effectiveness of single- versus triple-dose gadodiamide injection-enhanced MR angiography of the abdomen: a phase III double-blind multicenter study. Radiology 2001;219:137–46.

JACC: CARDIOVASCULAR IMAGING, VOL. 2, NO. 4, 2009
APRIL 2009:412–20

20. Pearson K III. Regression, heredity, and panmixia. Mathematical contributions to the theory of evolution. London, UK: Philosophical Transactions of the Royal Society of London, 1896:253–318.
21. Bland JM, Altman DG. Statistical methods for assessing agreement between two methods of clinical measurement. Lancet 1986;1:307–10.
22. Westgard JO, Hunt MR. Use and interpretation of common statistical tests in method-comparison studies. Clin Chem 1973;19:49–57.
23. Conover W. Practical Nonparametric Statistics. 2nd edition. New York, NY: John Wiley, 1980.
24. Ruzsics B, Suranyi P, Kiss P, et al. Automated multidetector computed tomography evaluation of subacutely infarcted myocardium. J Cardiovasc Comput Tomogr 2008;2:26–32.
25. Nieman K, Shapiro MD, Ferencik M, et al. Reperfused myocardial infarction: contrast-enhanced 64-section CT in comparison to MR imaging. Radiology 2008;247:49–56.

Key Words: computed tomography ■ myocardial infarction ■ radiation ■ viability ■ perfusion.